Mohammad Mansouri, Aly Abdelmagid, Zlata Tošić, Marta Orszt, Ahmed Elshafei

Corresponding Principal and Asymptotic Patches for Negatively-Curved Gridshell Designs

Abstract: A design model for negatively-curved gridshells whose primary and secondary structures are corresponding principal and asymptotic patches is presented. This correspondence is realized on minimal surfaces with their adjoint transform and on constant negative Gaussian curvature surfaces with their Bäcklund transforms. Based on the design model, we introduce a gridshell prototype utilizing the correspondence.

1 Introduction

It is known that principal patches have the advantage of giving rise to developable beams (ribs) as well as being the smooth continuous analogue of circular planar quadrilateral meshes cf. (Liu et al. 2006), (Abdelmagid et al. 2022) and (Bobenko and Tsarev 2007). Asymptotic patches, on the other hand, have the advantage of generating ribs that unroll (albeit with some deformation) to almost straight bands (Jiang et al. 2020). Thus having a viable model to associate them is beneficial for design purposes, more precisely that the two are diagonal to one another (in domains). From another side, it is also known that structural bracing in the sense of two intersecting grids defining a primary and a secondary structure is essential in gridshell design. In the article, we present a design model consisting of three degrees of design freedom through which the designer can generate a wide variety of morphological solutions, all of which maintain the correspondence between principal-asymptotic patches. Finally, we present a gridshell prototype whose primary and secondary structures are from the corresponding principal and asymptotic patches.

2 Geometry

Let us recall some facts from differential geometry cf. (Eisenhart 1909) and (Gray et al. 2006). In all that follows, we denote by $X(u, v)$ a parameterization patch on a smooth negatively-curved surface S in three-dimensional space $\mathbb{R}^3$ equipped with the Euclidean scalar product $\langle , \rangle$. We denote by $X_u, X_v, X_{uu}, \ldots$ the partial derivatives and

https://doi.org/10.1515/9783111162683-005

by N the normal to S. The fundamental coefficients are given by

$$\begin{cases} F = \langle X_u, X_v \rangle \quad , \quad E = \langle X_u, X_u \rangle \quad , \quad G = \langle X_v, X_v \rangle \\ f = \langle X_{uv}, N \rangle \quad , \quad e = \langle X_{uu}, N \rangle \quad , \quad g = \langle X_{vv}, N \rangle \, . \end{cases} \tag{1}$$

2.1 Principal and asymptotic patches

We recall that a curve in a surface S is said to be principal if it is always tangent to a direction of principal curvature of S and is asymptotic if it has a vanishing normal curvature everywhere. Observe that the normals N along a principal curve form a developable strip, as seen in Fig. 1a. However, the normals along an asymptotic curve form a strip that unrolls (with deformation) to an almost straight band, as seen in Fig. 1b. Furthermore, a patch $X(u, v)$ on S is called principal (or orthogonal conjugate (OC)) if its coordinate lines are principal curves while a patch $Y(x, y)$ on S is asymptotic (or AS) if its coordinate lines are asymptotic curves. OC-patches are advantageous in giving rise to planar panels and orthogonal nodes.

$$\text{OC-patch:} \quad F_X = 0, f_X = 0 \tag{2}$$

$$\text{AS-patch:} \quad e_Y = 0, g_Y = 0. \tag{3}$$

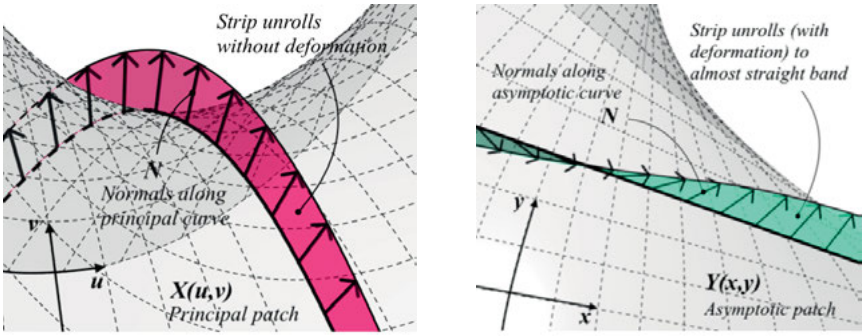

(a) (b)

Fig. 1: Behavior of normal strips along principal and asymptotic curves: (a) normals along principal, (b) normals along asymptotic.

2.2 Corresponding principal and asymptotic patches

We define the notion of correspondence between patches $X(u, v)$ and $Y(x, y)$ on the negatively-curved surface S to be given by (the linear change of coordinates) reparame-

terizations of the form

$$X(x+y, x-y) = Y(x,y) \quad \longleftrightarrow \quad X(u,v) = Y\left(\frac{u+v}{2}, \frac{u-v}{2}\right). \tag{4}$$

This construction establishes that the coordinate lines of the two patches are diagonal to one another in the parameter space, hence intersecting on S at exact points (corresponding to square lattices in the domains), as seen in Fig. 2. Observe that the reparameterization (4) creates a correspondence in the above sense between the following patches (described by their fundamental coefficients)

(C1) Y Iso-speed $(E_Y = G_Y)$ $\longleftrightarrow$ X Orthogonal $(F_X = 0)$

(C2) Y Conformal $(F_Y = 0, E_Y = G_Y)$ $\longleftrightarrow$ X Conformal $(F_X = 0, E_X = G_X)$

(C3) Y Tcheb-1 $(E_Y = G_Y = c)$ $\longleftrightarrow$ X Tcheb-2 $(F_X = 0, E_X + G_X = c)$

(C4) Y Asymptotic $(e_Y = g_Y = 0)$ $\longleftrightarrow$ X Iso-conjugate $(f_X = 0, e_X = -g_X)$

where c is a constant. There follows that combining any of the correspondences $C1, C2, C3$ with $C4$ yields a correspondence between principal and asymptotic networks on S, a property that in general is not true. More precisely, we have

$$\begin{array}{rcl} Y(x,y) & \longleftrightarrow & X(u,v) \\ \text{Iso-speed Asymptotic} & \longleftrightarrow & \text{Orthogonal Iso-conjugate.} \end{array}$$

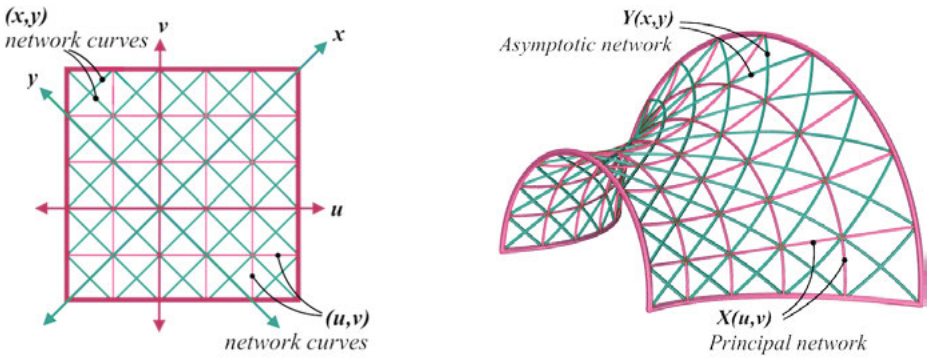

Fig. 2: Correspondence of principal and asymptotic networks: (a) intersecting in domain, (b) intersecting in surface.

2.3 Surfaces admitting principal-asymptotic correspondence

After defining the conditions for the correspondence, the following two realizations illustrate the combining of one the correspondences $C1, C2, C3$ with the correspondence $C4$.

Minimal Surfaces (MS) (C2 + C4)

The first type is the minimal surface (MS). The idea is to construct conformal iso-conjugate MS patches X starting from a conformal parameterization N of the sphere. We observe that when X is a conformal MS patch, its normal N is also conformal and it satisfies $e_X = -g_X$. Hence, the Codazzi equations reduce to the Cauchy-Riemann equations

$$\begin{cases} e_v = f_u \\ e_u = -f_v \end{cases} \quad \text{equivalently} \quad f_{uu} + f_{vv} = 0. \tag{5}$$

A general solution is given by two functions $\phi(u + iv)$ and $\psi(u - iv)$ such that

$$\begin{cases} f = \phi + \psi \\ e = -i(\phi - \psi) + c \end{cases}$$

where c is a constant and the quantity e is real when ϕ and ψ are complex conjugates. Thus, to each ϕ, ψ corresponds a conformal iso-conjugate MS patch X satisfying the differential system

$$X_u = -\frac{eN_u + fN_v}{\widetilde{\Lambda}}, \quad X_v = -\frac{fN_u - eN_v}{\widetilde{\Lambda}} \tag{6}$$

where $\widetilde{\Lambda}$ is the conformal factor of N. Precisely, if we take f equals 0 and e equals 1, then a solution $X(u, v)$ to Eq. (6) is conformal iso-conjugate, as seen in Fig. 3a and its corresponding reparameterization using (4) yields a conformal asymptotic patch $Y(x, y)$, as seen in Fig. 3b.

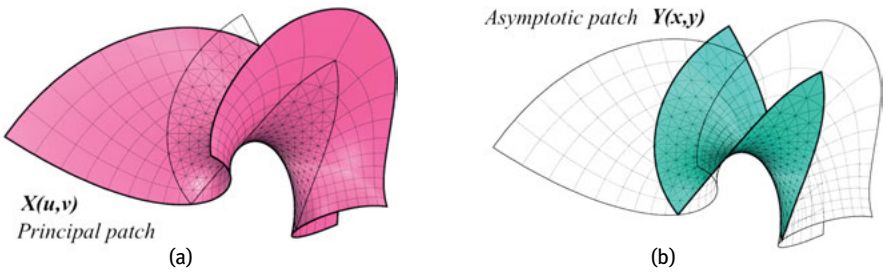

Fig. 3: Principal-Asymptotic correspondence realized on MS: (a) principal patch on MS, (b) asymptotic patch on MS.

Constant negative Gaussian curvature (CGC) surfaces (C3 + C4)

The second type of principal-asymptotic correspondence is in the context of surfaces of negative CGC. Recall that a surface S with negative CGC equals to $-1/\rho^2$ for $\rho > 0$

admits a Tcheb-2 iso-conjugate patch $X(u, v)$ characterized by

$$\begin{cases} F_X = 0\,, \quad E_X + G_X = (\rho\cos\theta)^2 + (\rho\sin\theta)^2 = \rho^2 \\ f_X = 0\,, \quad e_X = -g_X = \pm\rho\sin\theta\cos\theta \end{cases}$$

with angle function $\theta(u, v)$ satisfying the Sine-Gordon-2 equation

$$\theta_{uu} - \theta_{vv} = \sin\theta\cos\theta. \tag{7}$$

The function θ can be understood geometrically as half the angle ω between the asymptotic directions, and the Sine-Gordon equation (7) arises directly from using the expressions of the fundamental coefficients in the Gauss-Codazzi equations. Therefore, the corresponding reparameterization using Eq. (2) thus yields a Tcheb-1 asymptotic patch $Y(x, y)$ characterized by

$$\begin{cases} F_Y = \rho^2\cos\omega \;\;, \quad E_Y = G_Y = \rho^2 \\ f_Y = \mp\rho\sin\omega \;\;, \quad e_Y = g_Y = 0 \end{cases}$$

with angle function $\omega(x, y)$ satisfying the Sine-Gordon-1 equation

$$\omega_{xy} = \sin\omega. \tag{8}$$

We focus, in particular, on the Pseudo-Sphere (PS), Dini surface, and Kuen surface as seen in Fig. 4. The explicit parameterizations $X(u, v)$ of the surface in question are obtained by Bäcklund transformations explained in the next section.

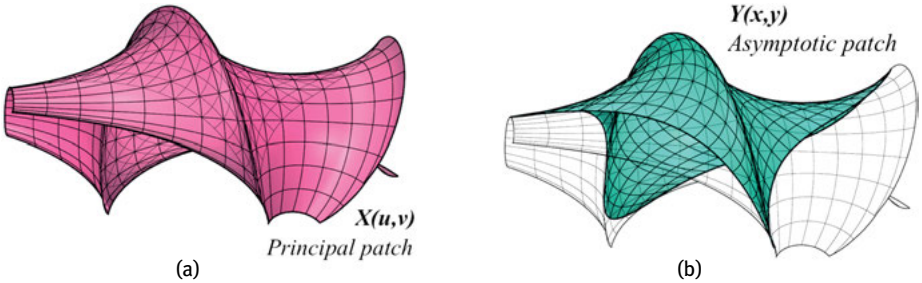

Fig. 4: Principal-Asymptotic correspondence realized on negative CGC: (a) principal patch on CGC, (b) asymptotic patch on CGC.

2.4 Transformations preserving the correspondence

Next, we present surface transformations that preserve the principal-asymptotic correspondence. For that, we need the transformation to preserve the orthogonality and

iso-conjugacy of $X(u, v)$ (or equivalently the iso-speed and asymptotics of $Y(x, y)$), in the types of surfaces specified above. In this context, we present transformations only for surface type B (MS) namely, the adjoint transformation, and for surface type C (Negative CGC) namely, the Bäcklund transformation.

Adjoint transformation

To understand this transformation, we consider the Eqs. (6). We saw above that we chose f to be 0 and e to be 1, reducing the system to Eqs. (9) and obtaining a solution $X(u, v)$ which is a conformal iso-conjugate MS patch. Now, if we instead take f to be 1 and e to be 0, reducing the system to Eqs. (10) and thus obtaining a solution $X^*(u, v)$ which is a conformal asymptotic MS patch.

$$X_u = -\frac{N_u}{\widetilde{\Lambda}}, \quad X_v = \frac{N_v}{\widetilde{\Lambda}} \tag{9}$$

$$X_u^* = -\frac{N_v}{\widetilde{\Lambda}}, \quad X_v^* = -\frac{N_u}{\widetilde{\Lambda}}. \tag{10}$$

It can be seen that X and X^* are related by with Cauchy-Riemann equations

$$X_u = X_v^*, \quad X_v = -X_u^*. \tag{11}$$

thus are called adjoints of one another, as seen in Fig. 5. Finally, the conformal iso-conjugate patch $Y^*(x, y)$ is adjoint to the conformal asymptotic patch $Y(x, y)$.

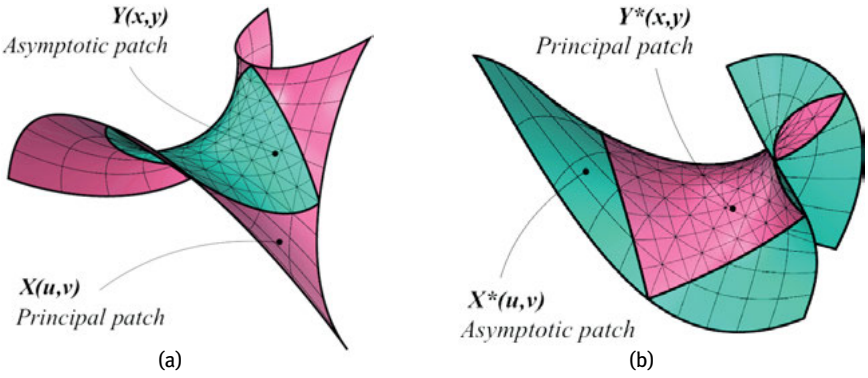

Fig. 5: MS surface and its adjoint transform MS: (a) X principal and Y asymptotic, (b) X^* asymptotic and Y^* principal.

Bäcklund transformation

The Bäcklund transform of a surface S with negative CGC $-1/\rho^2$ for $\rho > 0$ is a surface S^* of the same negative CGC defined as the locus of points drawn by moving a line L over the points of S. This line L is tangent to both surfaces and is of constant length $\rho \cos\sigma$, for some real constant σ. Moreover, the normals to S and S^* make a constant angle together of $(\pi/2 - \sigma)$. In particular, when σ is 0, the surface S^* is said to be a Bianchi transform, as seen in Fig. 6. Now, if S of negative CGC equals $-1/\rho^2$ defined by a Tcheb-2 iso-conjugate patch $X(u, v)$ of angle function $\theta(u, v)$, its Bäcklund transformation is given by

$$X^*(u,v) = X(u,v) + \left(\frac{\cos\sigma\cos\theta^*}{\cos\theta}\right) X_u + \left(\frac{\cos\sigma\sin\theta^*}{\sin\theta}\right) X_v \tag{12}$$

where the angle function $\theta^*(u, v)$ satisfying the Bäcklund-Darboux system

$$\begin{cases} \theta^*_u + \theta_v = \sec\sigma\,(\sin\theta^*\cos\theta + \sin\sigma\cos\theta^*\sin\theta) \\ \theta^*_v + \theta_u = -\sec\sigma\,(\cos\theta^*\sin\theta + \sin\sigma\sin\theta^*\cos\theta)\,. \end{cases} \tag{13}$$

In this context, we give the explicit Tcheb-2 iso-conjugate patches $X(u, v)$ for the PS, Dini, and Kuen surfaces as Bäcklund (and Bianchi) transformations. More precisely, the PS is obtained as a Bianchi transformation of the vertical line (which can be seen as a degenerate surface), and the Dini surface as a Bäcklund transformation of the vertical line. Finally, the Kuen surface is given as a Bianchi transformation of the PS, note that all these surfaces have negative CGC $-1/\rho^2$.

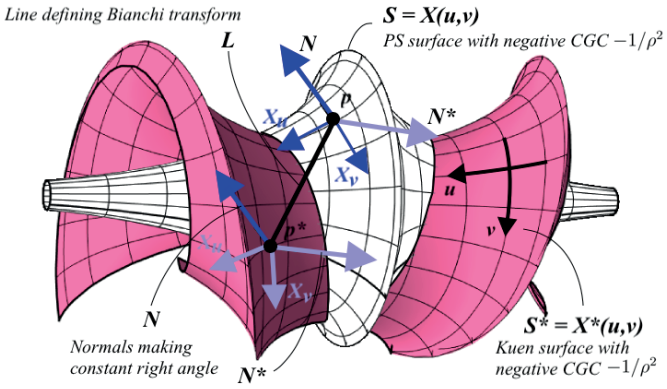

Fig. 6: Bäcklund (in fact Bianchi) transform of PS to Kuen surface.

3 Design Model

Now we explain how the geometric constructions described above are reinterpreted as three Degrees of Design Freedom (DF) constituting the design model

- **DF-1:** Surface type
- **DF-2:** Subtypes
- **DF-3:** Variations and transformations.

DF-1 is the choice of one of two surface types explained above (A) Minimal surface or B) Negative CGC). Once a surface type is chosen, DF-2 generates subtypes through different ways of constructing the surface type in question. Finally, DF-3 provides variations and transformations by manipulating the different parameters in their equations. Note that DF-3 preserves the surface type and the correspondence. In the following part, we show the generation of two subtypes for surface type A (MS) and one subtype for surface type B (Negative CGC).

Surface type A (MS)

Subtype A01

Conformal N obtained by composing the holomorphic function $f(z) = (az + b)/(cz + d)$ where a, b, c, d are reals such that $ad \neq bc$, with the inverse of the stereographic projection, the variations of the resulting subtype (Fig. 7) is obtained by manipulating the parameters a, b, c, d in:

$$\frac{1}{6(ad-bc)}\begin{pmatrix} 3b^2u - 3d^2u + (a^2-c^2)u(u^2-3v^2) + 3ab(u^2-v^2) + 3cd(v^2-u^2) \\ v(3b^2 + 3d^2 + 6abu + 6cdu + (a^2+c^2)(3u^2-v^2)) \\ -6bdu - 2acu(u^2-3v^2) - 3bc(u^2-v^2) - 3ad(u^2-v^2) \end{pmatrix}$$

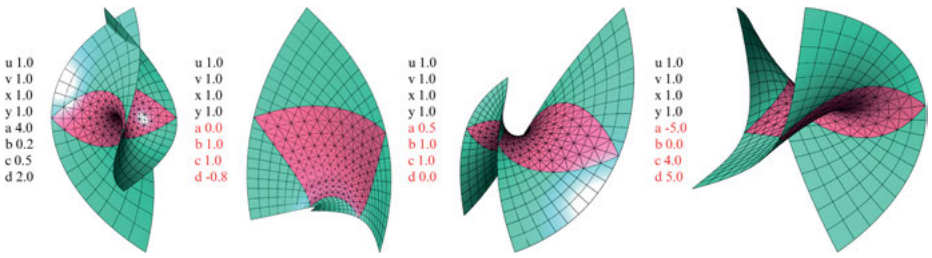

Fig. 7: Variations of Subtype A01.

The transformation (preserving the surface type and the OC-AS correspondence) is provided by the expression for the adjoint MS patches X^*, Y^* explained above.

Subtype A02

Conformal N obtained by composing the holomorphic function $f(z) = \alpha z^2$ where $\alpha = a + ib$, with the inverse of the stereographic projection, the variations of the subtype (Fig. 8) are obtained by manipulating the parameters a, b in:

$$\frac{1}{16(a^2+b^2)}\begin{pmatrix} (a^2+b^2)\left(4buv(v^2-u^2)+a(u^4-6u^2v^2+v^4)\right)-4b\arctan\left(\frac{v}{u}\right)-2a\log(u^2+v^2) \\ (a^2+b^2)\left(4auv(u^2-v^2)+b(u^4-6u^2v^2+v^4)\right)+4a\arctan\left(\frac{v}{u}\right)-2b\log(u^2+v^2) \\ 4(v^2-u^2)(a^2+b^2) \end{pmatrix}$$

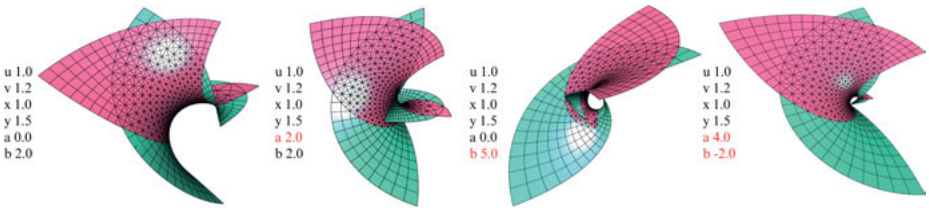

Fig. 8: Variations of subtype A02.

Surface type B (Negative CGC)

In this surface type, the subtypes are essentially the PS, Dini, and Kuen surfaces obtained as Bäcklund transforms. Notice that solving the Bäcklund-Darboux Eq. (13) gives us a constant of integration w, which creates a family of solutions seen as variations in the subtype (Fig. 9). Next, varying the angle σ (between 0 and $\pi/2$) results in different Bäcklund transforms, while the parameter ρ controls the general negative CGC of the surfaces.

Subtype B01

This subtype is obtained as a Bäcklund transform of the vertical line, and its variations are obtained by manipulating ρ, σ, w. In particular, when $\sigma = 0$ we obtain the PS.

$$\rho\left(\frac{\cos\sigma\cos v}{\cosh(u\sec\sigma - v\tan\sigma + w)}, \frac{\cos\sigma\sin v}{\cosh(u\sec\sigma - v\tan\sigma + w)}, u - \cos\sigma\tanh(u\sec\sigma - v\tan\sigma + w)\right)$$

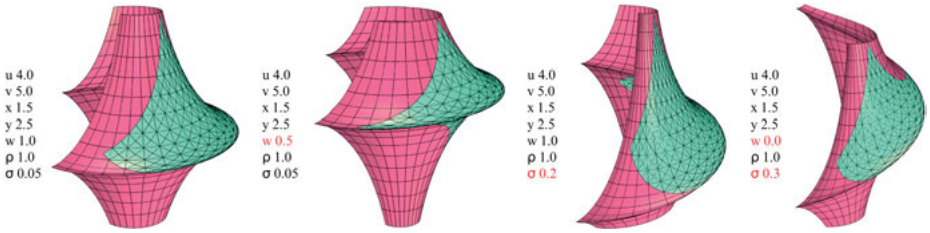

Fig. 9: Variations of Subtype B01.

4 Design application (Gridshell design)

Next, we present a gridshell prototype based on a variant of subtype A01 (surface type MS), where DF-1, DF-2, and DF-3 are used to generate the form and the structural/architectural elements utilizing the principal-asymptotic correspondence.

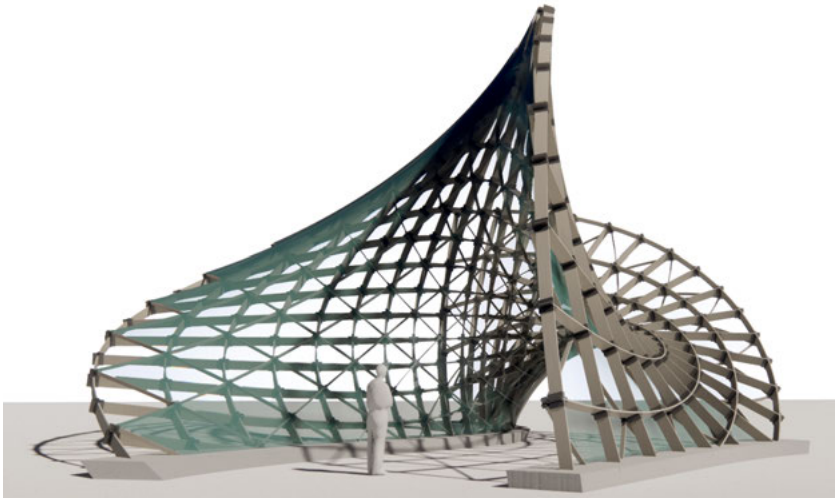

Fig. 10: Design prototype for a gridshell.

Elements assembly

In Fig. 11, we see a zoom-in on a detail from the proposed gridshell prototype that shows the assembly of the stacked ribs from the two patches (which generate the primary and secondary structures), the connector, and the quad panels.

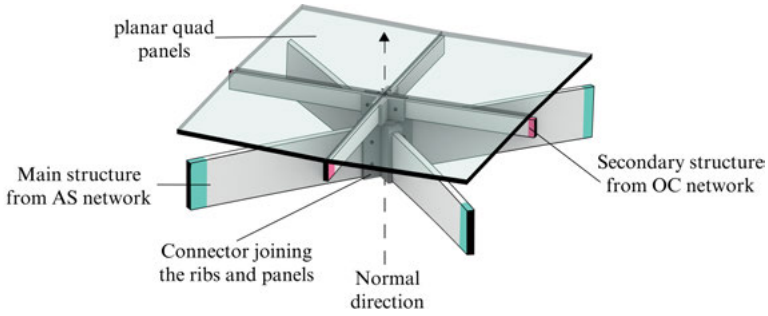

Fig. 11: Assembly of the three elements.

Element 01 (Ribs)

As shown in Fig. 12, both sets of ribs are generated from strips arising from the normals along their respective network curves. The ribs of the primary structure are from the asymptotic network, which unroll (albeit with deformation) to almost straight bands, cf. (Jiang et al., 2020). While the ribs of the secondary structure are from the principal network which are naturally developable. The two directions of each set of ribs are joined through a slit assembly to maintain the continuity of the ribs.

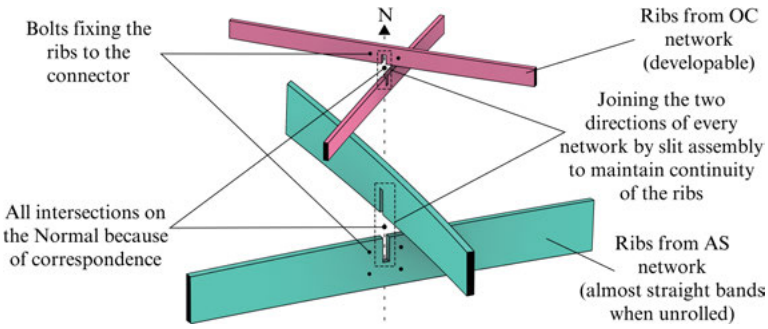

Fig. 12: Main and secondary structures.

Element 02 (Connector)

Since the strips forming the ribs in question are generated by the normals, their intersections will always coincide with the normal direction. Hence, simplifying the design of the connector joining all the elements of the structure, as seen in Fig. 13.

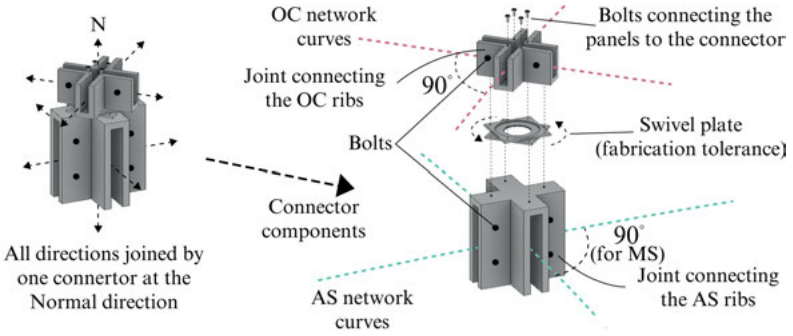

Fig. 13: Connector.

Element 03 (Quad panels)

Recall that OC-patches are the continuous smooth analogues of circular quad meshes. Thus, we can use planar quad panels (up to architectural tolerance) in our construction. These panels provide cladding and secondary bracing of the structure. The panels are bolted to the OC-joint at the normals, as seen in Fig. 11.

5 Conclusion

In this work, we presented a geometric setting for the correspondence between principal and asymptotic patches on surfaces of constant negative Gaussian curvature. That is since, on one hand, principal and asymptotic patches provide advantages for architecture fabrication. On the other hand, intersecting grids are structurally beneficial for grid shells, especially when these grids are principal and asymptotic networks. It is important to point out that the design model presented here provides an accessible way to realizing principal-asymptotic correspondence on two surface types and their variants, which is not a generically true condition. Moreover, the model created parameter spaces of rationalized morphological explorations that respect the geometric conditions of the correspondence. Finally, we presented a prototype of the morphological options.

Acknowledgements

The research of the fifth author Elshafei, A. was partially financed by Portuguese Funds through FCT (Fundação para a Ciência e a Tecnologia) within the Projects UIDB/00013/2020 and UIDP/00013/2020. The work of the fourth author Orszt, M. is financed by national funds through FCT - Fundação para a Ciência e a Tecnologia, I.P., under the Strategic Project with the references UIDB/04008/2020 and UIDP/04008/2020.

The research of third author Tošić, Z. is a part of the priority program SPP 2187: Adaptive Modular Construction with Flow Production Methods – Precision High-Speed Construction of the Future in the subproject Formwork-free Flow Production of Adaptive Supporting Structures from Variable Frame Elements – Adaptive Concrete Diamond Construction (ACDC) funded by the German Research Foundation (DFG).

References

Abdelmagid, A., Elshafei, A., Mansouri, M., and Hussein, A. (2022). A design model for a (grid)shell based on a triply orthogonal system of surfaces. In *Towards Radical Regeneration: DMS Berlin 2022*. Springer.

Bobenko, A. and Tsarev, S. (2007). Curvature line parameterization from circle patterns. https://arxiv.org/abs/0706.3221

Eisenhart, L. (1909). *A Treatise on Differential Geometry of Curves and Surfaces*. Ginn and Company, Boston.

Gray, A., Abbena, E., and Salamon, S. (2006). *Modern differential geometry of curves and surfaces with Mathematica*. 3rd Edition. Chapman & Hall/CRC.

Jiang, C., Wang, C., Schling, E., and Pottmann, H. (2020). Computational design and optimization of quad meshes based on diagonal meshes. *In Advances in Architectural Geometry 2020*. Springer.

Liu, Y., Pottmann, H., Wallner, J., Yang, Y., and Wang, W. (2006). Geometric modeling with conical meshes and developable surfaces. *ACM Tr., Proc. SIGGRAPH,* 25 (3): 681–89.